Available online at www.sciencedirect.com
ScienceDirect
Earth and Planetary Science Letters 249 (2006) 241 – 257
EPSL
www.elsevier.com/locate/epsl

Chicxulub impact event is Cretaceous/Paleogene boundary in age: New micropaleontological evidence

Ignacio Arenillas [a,*], José A. Arz [a], José M. Grajales-Nishimura [b], Gustavo Murillo-Muñetón [b], Walter Alvarez [c], Antonio Camargo-Zanoguera [d], Eustoquio Molina [a], Carmen Rosales-Domínguez [b]

[a] *Departamento de Ciencias de la Tierra (Paleontología), Universidad de Zaragoza, 50009 Zaragoza, Spain*
[b] *Instituto Mexicano del Petróleo (Exploración y Producción), Eje Lázaro Cárdenas # 152, Mexico D.F., 07730, Mexico*
[c] *Department of Earth and Planetary Science, University of California, 307 McCone Hall, Berkeley, CA 94720-4767, USA*
[d] *Petróleos Mexicanos, Exploración y Producción (retired), Blvd. A. Ruiz Cortines 1202, Villahermosa, Tabasco, 86030, Mexico*

Received 18 February 2006; received in revised form 1 July 2006; accepted 12 July 2006
Available online 17 August 2006
Editor: M.L. Delaney

Abstract

High-resolution and quantitative planktic foraminiferal biostratigraphy from two SE Mexico stratigraphic sections (Bochil, Guayal) shows that the Chicxulub-related Complex Clastic Unit (CCU) is synchronous with the ejecta-rich airfall layer and the Cretaceous/Paleogene (K/Pg) catastrophic mass extinction horizon in the El Kef (Tunisia) and Caravaca (Spain) sections. The lowermost Danian *H. holmdelensis* subzone (=Biozone P0) was identified in both sections in a thin dark clay bed just above the CCU, proving that such bed is chronostratigraphically equivalent to the K/Pg boundary clay of the El Kef stratotype. These new micropaleontogical data confirm that the K/Pg impact event and the Chicxulub impact event are the same one. This contradicts the suggestion by others that the Chicxulub impact predated the K/Pg boundary by about 300 ka.

Keywords: Planktic foraminifera; Biochronology; Acme stages; K/Pg clay; Impact crater

1. Introduction

The 65 Ma-old Cretaceous/Paleogene (K/Pg) mass extinction appears to have been a catastrophic event related to the aftermaths of a ~10 km-diameter asteroid impact [1,2]. Dust and fine ejecta covered the atmosphere and were deposited slowly, probably over months or a few years, forming a millimeter-thick airfall layer worldwide [3,4]. This layer contains evidence of the meteoritic impact including: an iridium anomaly, siderophile trace elements in chondritic proportions, osmium and chromium isotope anomalies, microdiamonds, nickel-rich spinels, shocked quartz, and altered microtektites [5–8]. It is placed at the basal part of a dark clay bed commonly called the “K/Pg boundary clay”, which was deposited during a global decrease in ocean productivity after the meteorite impact [9]. The K/Pg boundary was formally defined at the base of this dark clay in the K/Pg Global Stratotype Section and Point at

* Corresponding author. Tel.: +34 976 762475; fax: +34 976 761106.
E-mail address: ias@unizar.es (I. Arenillas).

0012-821X/$ - see front matter © 2006 Elsevier B.V. All rights reserved.
doi:10.1016/j.epsl.2006.07.020

El Kef (Tunisia), i.e., at the base of the airfall layer containing the impact material [10,11], and coincides with the planktic foraminiferal catastrophic mass extinction [5,12]. According to that definition, all the impact material overlies the K/Pg boundary and the lithological unit containing this material is consequently Danian in age.

The K/Pg boundary impact site was located in the northern Yucatan Peninsula (Mexico) [13] after recognition of a ~180 km-wide crater, whose center lies below the small town of Puerto Chicxulub [14]. Impact sequences in boreholes drilled within the Chicxulub crater are characterized by impact melt and suevite breccias. Those were dated with the ^{40}argon/^{39}argon method to be approximately 65 Ma [15,16], supporting a genetic link between the Chicxulub impact and the K/Pg boundary. The genetic links between the ejecta and the crater are also indicated by the isotopic compositions of the glass [17] or shocked zircons dating [18]. In Gulf of Mexico and Caribbean sections, the K/Pg sequence outside the crater is represented by a characteristic impact material-rich Complex Clastic Unit (CCU). The chemical composition of fresh impact glass fragments from the CCU at Beloc (Haiti) and El Mimbral (NE Mexico) is similar to that of the Chicxulub melt rock, indicating that the three sequences are genetically related [19]. Those impact glasses were also dated as 65.07±0.1 Ma, based on the ^{40}Ar/^{39}Ar method [16]. However, isotopic dating commonly has a margin of error which does not provide enough resolution to test whether there is an exact coincidence in time between the Chicxulub impact and the K/Pg extinction event.

As a result, the high resolution of planktic foraminiferal biozones has been used to pinpoint the age of the Chicxulub impact. Based on this method, some scientists have argued that the Chicxulub impact occurred about 300 ka before the K/Pg boundary [20]. According to their "ultraimpactist" scenario, the K/Pg crater has yet to be found, and Chicxulub is just one of the several impact events that arose across the K/Pg boundary over a period of 400 ka. This controversial hypothesis contradicts the detailed Ir profile for 10 Ma across the K/Pg boundary performed at Gubbio (Italy), where only one Ir anomaly was identified right at the boundary [21], in addition to micropaleontological and sedimentological evidence from most continuous Tethyan sections, such as Caravaca (Spain) and El Kef, which indicate only one impact event [5,12,22].

Much research has shown that Chicxulub has an age corresponding to the K/Pg boundary, including multidisciplinary studies in Mexican and Caribbean CCUs [11,23–27]. Nevertheless, no continuous K/Pg sections have been discovered yet in those areas. Based on high-resolution planktic foraminiferal biostratigraphy, two recognizable hiatuses were identified in sections from northern Mexico and Cuba, at the uppermost Cretaceous and the lowermost Paleocene [28–30]. Recently, the Yaxcopoil-1 well was drilled within the Chicxulub crater to determine its role in the K/Pg event. However, the presence of two similar hiatuses (affecting the upper part of the Maastrichtian and the lower part of the Danian) has raised a debate, since some researchers continue claiming that Chicxulub is not K/Pg in age [31], in disagreement with other investigators [32,33]. Detailed analysis of continuous marine K/Pg sections rich in planktic foraminifera near the impact site will help to resolve the controversy.

In this study, a micropaleontological and sedimentological analysis to establish if the Chicxulub event coincides with the planktic foraminiferal mass extinction and the K/Pg boundary is conducted. A high-resolution planktic foraminiferal biostratigraphical analysis at the K/Pg Bochil and Guayal sections was performed for the first time, and correlated to those obtained from the El Kef and Caravaca sections.

2. Location and sedimentological setting

The studied sections in this work are located in southeastern Mexico. The Bochil section (17°00′43" N, 92°56′50" W) is located in the State of Chiapas, about 9 km northeast from the town of Bochil, whereas the Guayal section (17°32′39" N, 92°36′80" W) is located in the State of Tabasco, about 60 km southeast of the City of Villahermosa. Both outcrops provide good exposures across more than 100 m and are two of the most representative southern Mexican K/Pg sections, relatively close to the Chicxulub crater (Fig. 1). There, the CCU is sandwiched between two pelagic formations rich in planktic foraminifera: the underlying Jolpabuchil Formation (Campanian–Maastrichtian) and the overlying Soyaló Formation (Paleocene).

The Chicxulub impact influenced strongly the sedimentary processes across the Gulf of Mexico and Caribbean regions. That event triggered intensive seismic activity and giant tsunamis that destabilized the continental margins and deposited CCUs in deep-water environments [11,27,30,34,35]. The thickness, lithology and sedimentology of those clastic deposits depend on their distance from the Chicxulub crater, their depositional environment (depth of deposition), and the origin of their allochthonous material (from the shelf and upper slope). Stratigraphic data from numerous southern Mexican sections and wells indicate that the local CCU has a

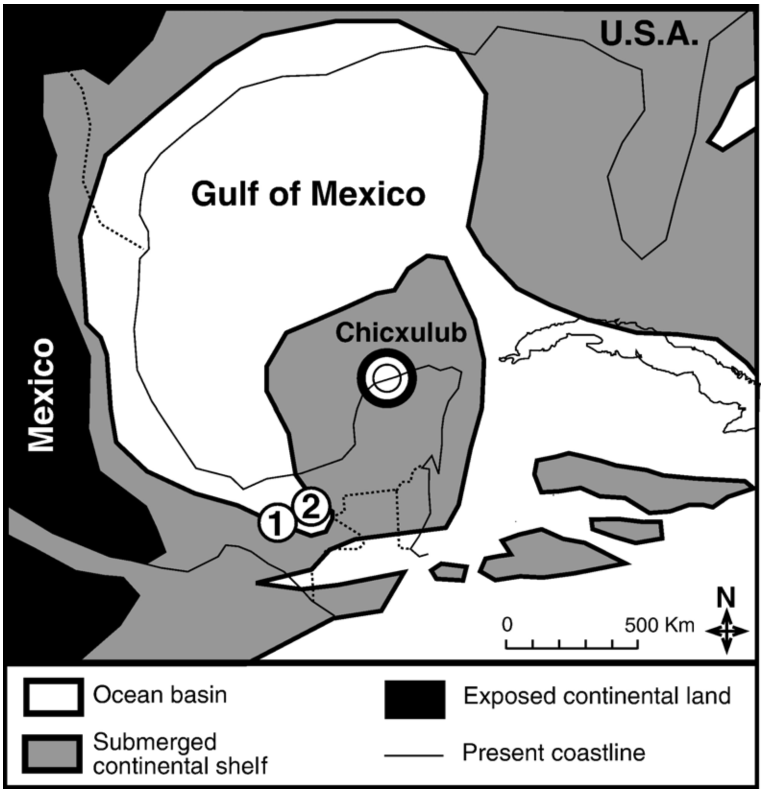

Fig. 1. Geographic and paleogeographic location of the K/Pg Bochil and Guayal stratigraphic sections and the Chicxulub crater (1: Bochil section; 2: Guayal section).

thick accumulation of coarse- and fine-grained carbonate breccias overlain by calcareous sandstones and fine ejecta [36,37].

The local CCU at Bochil and Guayal is a fining-upward sedimentary succession that can be subdivided, from base to top, into four distinct subunits [37]. Subunit 1 consists of a very coarse-grained carbonate breccia that grades to fine grained carbonate breccia; large limestone blocks up to 2 m in diameter are common in the basal part. Subunit 2 is a fine-grained calcareous breccia and coarse-grained calcareous sandstone mixed with scarce impact materials (e.g., shocked quartz, altered microtektites); the limestone fragments are only a few centimeters in diameter. Subunit 3 consists of very fine-grained yellow rippled sandstone and siltstone rich in ejecta constituents including shocked mineral phases, and distinctive accretionary lapilli at Guayal. Finally, Subunit 4 is a thin yellow–red shaly layer that represents the finest ejecta. This layer has a distinctive Ir anomaly, 1.5 ppb at Bochil and 0.8 ppb at Guayal [36,38].

A dark clay bed overlies the CCU at both Bochil and Guayal sections, and marks the base of the Soyaló Formation (Fig. 2). At Bochil, this bed is 6–8 cm thick with centimeter-intercalated layers of greenish-gray clays and reddish shales. At Guayal, it is a 3–4 cm thick dark greenish-gray clay with interbedded reddish shales in millimeter layers.

Sedimentological analyses suggest that the Bochil and Guayal CCUs represent a single graded, high-density flow deposit probably accumulated in hours, days or weeks, and partially reworked by megatsunami currents [26,39]. The allochthonous calcareous material of those CCUs was derived mainly from the adjacent Chiapas–Tabasco Platform. Limestone blocks contain common rudist and coral fragments, and reworked benthic larger foraminifera such as *Chubbina*. Microfacies identified in the lithoclasts of carbonate breccias are typical of three depositional environments: inner plaform, platform margin, and deep-water settings [37]. Only one horizon of bioturbation was identified in the Bochil and Guayal CCUs, corresponding with its uppermost centimeters (e.g., small isolated *Zoophycos* at Guayal, and *Chondrites* with a patched pattern at Bochil). This finding agrees with a period of low sedimentation rate after the rapid deposition of these CCUs, indicating bioturbation by Danian organisms. This horizon may be

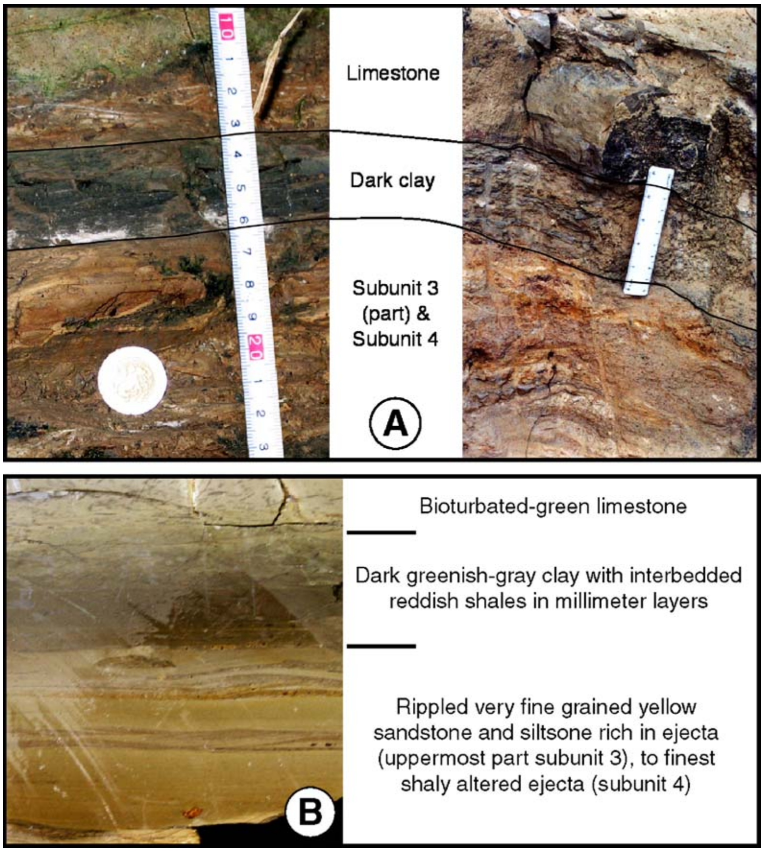

Fig. 2. (A) Field photographs of details of the K/Pg boundary clay bed and uppermost CCU subunits (3 and 4) at the Guayal (left) and Bochil (right) sections; (B): Polished-section of the uppermost 5 cm of the CCU and the lowermost 4 cm of the Soyaló Formation at Guayal. At both sections, the Ir-anomalous Subunit 4 is immediately below the dark clay.

correlated with the bioturbated horizon of the top of CCU in some K/Pg sections from northeastern Mexico [11] and Yaxcopoil-1 drill hole [32,33].

3. Planktic foraminiferal data

3.1. Methods

Sixty two samples at Bochil and sixty samples at Guayal across the critical K/Pg boundary interval were collected for micropaleontological analysis. The upper part of the CCU and the lowermost Danian stratigraphic interval were sampled at high-resolution, i.e., at centimeter-intervals (see Tables 1–3). The clay and marly samples were processed using standard disaggregating technique employing diluted H_2O_2. The remaining more lithified samples were processed using a technique recently proposed [40], which includes sample disaggregation in a solution with 80% acetic acid and 20% H_2O. All samples were dried at ≤ 50 °C, and sieved into 38–63 μm and ≥ 63 μm size fractions. In the Bochil section, except for the CCU, a split of >300 planktic foraminiferal specimens from ≥ 63 μm size fraction was picked from each Maastrichtian and Danian sample, using an Otto splitter. In the Bochil CCU and Guayal section, there were too few planktic foraminifera in the sample for quantitative studies. To find very infrequent species, the residue of all samples in size fractions larger than 38 and 63 μm was intensively scanned. Specimens were identified, sorted, and fixed on a standard 60-square micropaleontological slide.

3.2. Biozonations and Biochronology

The Maastrichtian and Danian Biozonations and Biochronology are based on previous planktic foraminiferal zonations and biochronological analysis for the middle and lower latitudes [22,41–45]. The rapid evolution and diversification of planktic foraminifera after the K/Pg mass extinction provides very high-resolution zonations in the lowermost Danian. This makes it possible to subdivide the standard biozones, i.e., *Guembelitria* *cretacea*, *Parvularugoglobigerina eugubina* and *Parasubbotina pseudobulloides* zones [46], into several subbiozones [22]. The *Guembelitria cretacea* zone was subdivided into the *Hedbergella holmdelensis* and *Parvularugoglobigerina longiapertura* subzones; the *Parvularugoglobigerina eugubina* zone into the *Parvularugoglobigerina sabina* and *Eoglobigerina simplicissima* subzones; and the *Parasubbotina pseudobulloides* zone into the the *Eoglobigerina trivialis* and *Subbotina triloculinoides* subzones. The highest stratigraphic records of *Abathomphalus mayaroensis* and *Plummerita hantkeninoides*, and the lowest stratigraphic records of *Parvularugoglobigerina longiapertura*, *Parvularugoglobigerina eugubina*, *Eoglobigerina simplicissima*, *Parasubbotina pseudobulloides* and *Subbotina triloculinoides* were the key biohorizons used to define the base of the different subzones such as what is shown in Fig. 3. The Fig. 3 also shows the Maastrichtian planktic foraminiferal biozonation used here [44], and the comparison with other biozonations [41,43,45].

The biostratigraphic interval between the K/Pg boundary and the first record of Danian species was

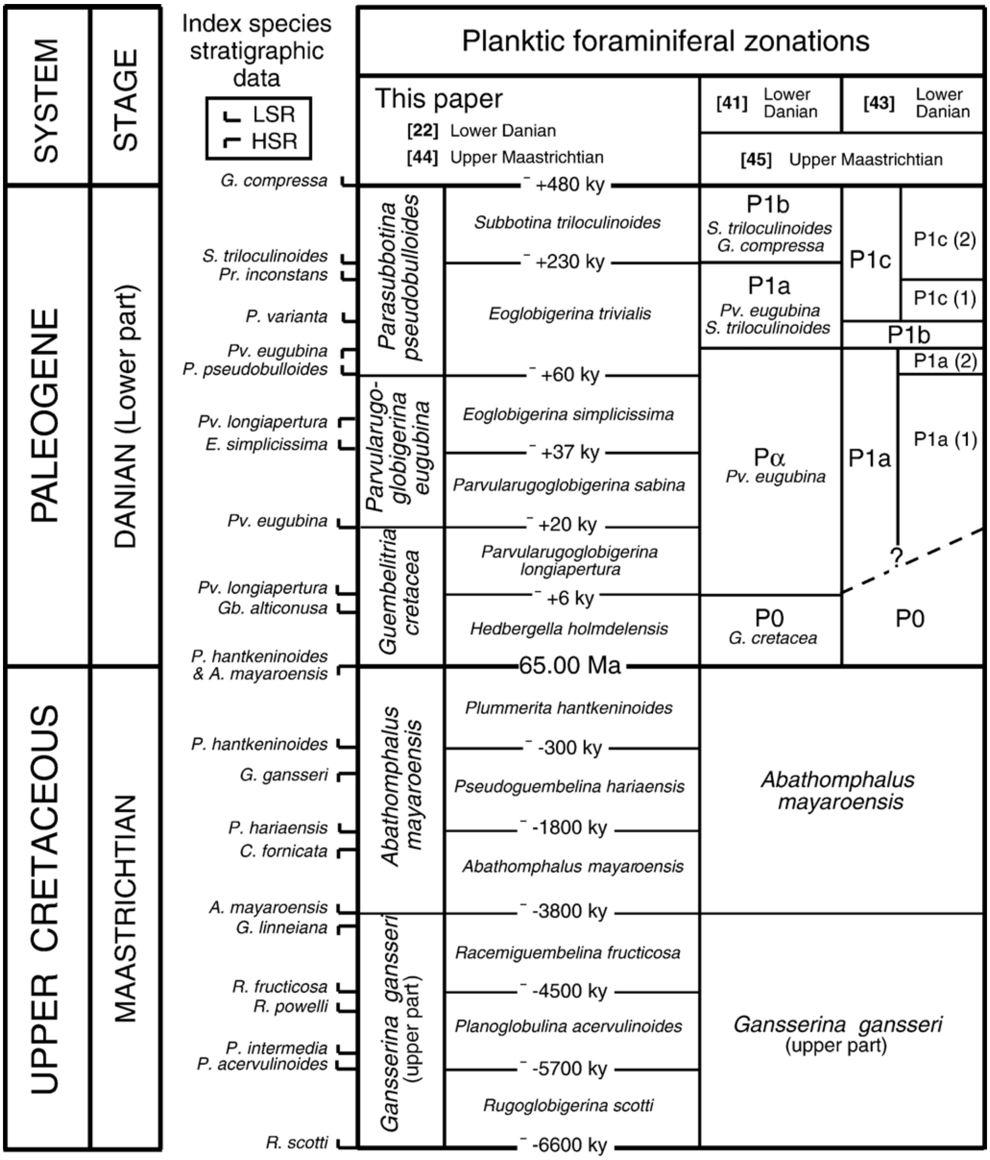

Fig. 3. Comparison of the planktic foraminiferal zonation used in this paper with other biozonations, the estimated ages of the biozonal boundaries, and stratigraphic data on several index species.

used to define the first, lowermost Danian planktic foraminiferal zone named P0 [5]. This biozone corresponds to the *H. holmdelensis* subzone [22], and spans the lower part of the K/Pg boundary clay bed at El Kef and other Tethyan sections. A recent biomagnetostratigraphic calibration at complete and very expanded Spanish sections such as Caravaca, Agost and Zumaya has made possible to estimate the age of the first appearance of the Danian index species and to calibrate the zonal boundaries [22]. The estimated ages of the biozonal boundaries are shown in Fig. 3. For example, the estimated duration of the *H. holmdelensis* subzone (=P0 Zone) is approximately 6 ka, which is shorter than the estimated duration for the K/Pg boundary clay deposition, about 10 ka, based on the near-constant flux of extraterrestrial helium-3 [47]. According to those biochronological data, the deposition of the 1–3 mm-thick ejecta layer at the El Kef stratotype (where the *H. holmdelensis* subzone spans 50 cm) occurred in an instantaneous geological time period [22].

3.3. Biostratigraphy and quantitative studies

The planktic foraminiferal assemblages in the uppermost 20 cm of autochthonous Maastrichtian marls (Jolpabuchil Formation) at Bochil are quite diverse and include 59 species (Table 1). The assemblages belong to the *Planoglobulina acervulinoides* subzone (upper part of the *Gansserina gansseri* zone). Likewise, the uppermost 14 m of autochthonous Maastrichtian limestones at the Guayal section contain 45 planktic foraminiferal species (Table 3) belonging to the *Racemiguembelina fructicosa* subzone (uppermost part of the *G. gansseri* zone). These data indicate a relevant erosional hiatus linked to the sudden emplacement of the CCU that affected the Upper Maastrichtian sediments (Fig. 3).

Isolated Maastrichtian planktic foraminiferal specimens were identified in the CCU of both sections, mainly in the breccia matrix of Subunit 1 and in the sandstone of Subunit 3 (Tables 1 and 3). Due to the allochthonous characteristics of the CCU material, we believe that all grains in the breccia matrix or in the sandstone are reworked, including the foraminiferal specimens. The age of emplacement of the CCU will be pointed out by its youngest microfossils among other evidence. Nevertheless, since the CCU at Bochil and Guayal only contain reworked microfossils, this stratigraphical interval cannot be assigned to any biozone, therefore it is included in a Barren Interzone (Fig. 4).

At Bochil and Guayal, the four lowermost Danian subzones (which span about the first 60 ka after the K/Pg boundary) were identified just above the CCU in the basal part of the Soyaló Formation. The thickness of these subzones at Bochil and Guayal are shown and compared with those of El Kef and Caravaca sections in Fig. 4. The *H. holmdelensis* subzone (=Biozone P0) is 5 cm-thick at Bochil and 3 cm-thick at Guayal, and contains oligotaxic assemblages composed mainly by *Guembelitria cretacea* and *G. trifolia*, as well as *H. holmdelensis*, *H. monmouthensis* and other possible Upper Maastrichtian survivors such as *Heterohelix globulosa*. This subzone is only slightly thinner than the dark bed clay (6–8 cm-thick at Bochil and 3–4 cm-thick at Guayal). The *P. longiapertura* subzone is 70 cm-thick at Bochil and 17 cm-thick at Guayal, and includes species such as *Parvularugoglobigerina longiapertura*, *Globoconusa alticonusa*, *Globoconusa fodina*, *G. cretacea*, *Woodringina claytonensis* and *Woodringina hornerstownensis*. The *P. sabina* subzone is 80 cm-thick at Bochil and 35 cm-thick at Guayal, and contains species such as *Parvularugoglobigerina eugubina*, *Parvularugoglobigerina sabina*, *P. longiapertura*, *G. alticonusa*, *G. fodina*, *G. cretacea*, *W. claytonensis*, *W. hornerstownensis*. Finally, the *E. simplicissima* subzone is 90 cm-thick at Bochil and 45 cm-thick at Guayal, and contains species such as *Eoglobigerina simplicissima*, *E. eobulloides*, *P. eugubina*, *G. fodina*, *Globonomalina archeocompressa*, *Chiloguembelina morsei*, *W. claytonensis*, *W. hornerstownensis*. These biostratigraphic data suggest that the lower Danian sedimentation rate at Guayal is similar to the one recorded at Caravaca (Fig. 4), whereas the sedimentation rate at Bochil is intermediate between the one of Caravaca and the one of El Kef [22]. The earliest Danian planktic foraminiferal evolutionary pattern was also documented at Bochil and Guayal (Tables 2 and 3), showing that the basal part of the Danian is continuous at both sections.

Quantitative studies in Spanish and Tunisian sections, such as Zumaya, Caravaca, Agost, El Kef, Aïn Settara or Elles, identified three planktic foraminiferal acme stages (PFAS 1–3) in the lower Danian related to the staged recovery of environmental conditions after the K/Pg boundary impact event [12,48–50]. The Bochil section is very rich in foraminifera, allowing a quantitative study of the lower Danian planktic foraminiferal assemblages (Table 2). The three acme stages were also identified at Bochil (Fig. 5): PFAS 1, dominated by *Guembelitria*, PFAS 2, dominated by *Parvularugoglobigerina* and *Globoconusa* species, and PFAS 3, dominated by *Woodringina* and *Chiloguembelina* species. The Fig. 5 shows a comparison of relative abundance of planktic foraminiferal groups and acme stages (PFAS) in the lowermost part of the Danian at the Bochil and El Kef sections. The evolution of the

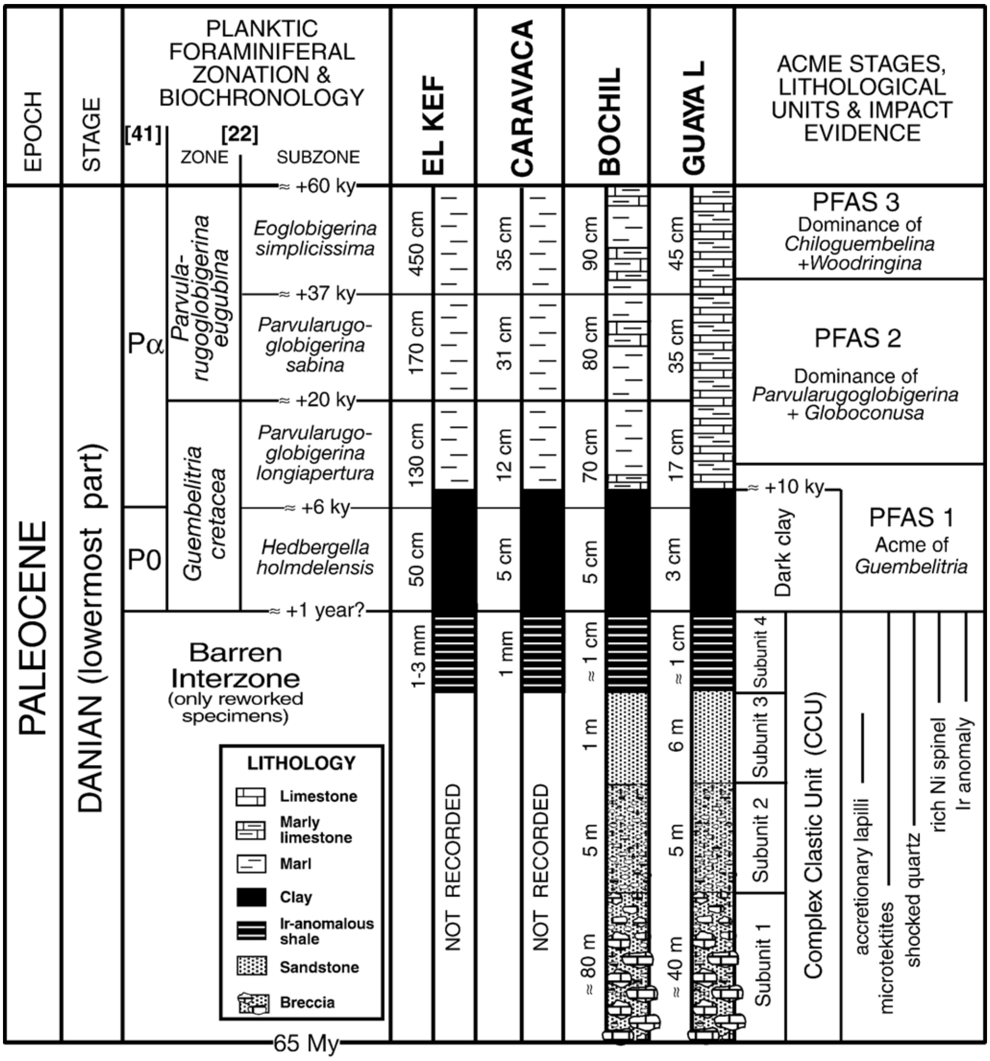

Fig. 4. Stratigraphic and biostratigraphic correlations of the El Kef, Caravaca, Bochil and Guayal sections, including the planktic foraminiferal zonations, thickness of each biozone in the four sections, key lithological beds across the K/Pg boundary, and thickness of the CCU subunits. At El Kef and Caravaca, the "K/Pg boundary clay" includes the Ir-anomalous shaly layer (airfall layer) and the dark clay. The dark clay bed is ≈100 cm thick at El Kef, 10–12 cm thick at Caravaca, 6–8 cm thick at Bochil, and 3–4 cm thick at Guayal.

planktic foraminiferal assemblages is similar in both sections suggesting that the lower Danian micropaleontological record at Bochil is as complete as at El Kef and other Tethyan sections.

4. Discussion

Using planktic foraminiferal biostratigraphic data from several sections in Mexico, Guatemala, Belize, and Haiti some authors [20] have suggested an impact multievent scenario in which three impact events happened across the K/Pg boundary. The first one, related to the CCU deposition and consequently the Chicxulub impact event, occurred about 300 ka before the K/Pg boundary. The second impact event corresponds to the well-known K/Pg event whose crater, according to those authors, is unknown. A third impact event occurred about 100 ka after the K/Pg boundary. This hypothesis contradicts the theory supported by most researchers that concluded, after analyses on these same sections and others (in USA and Cuba), that only one significant impact event is recorded in the Gulf of Mexico and Caribbean, and happened in coincidence with the K/Pg boundary [11,27,29,30,35,37,51–57].

The authors supporting the impact multievent hypothesis reported preliminary studies of the Bochil

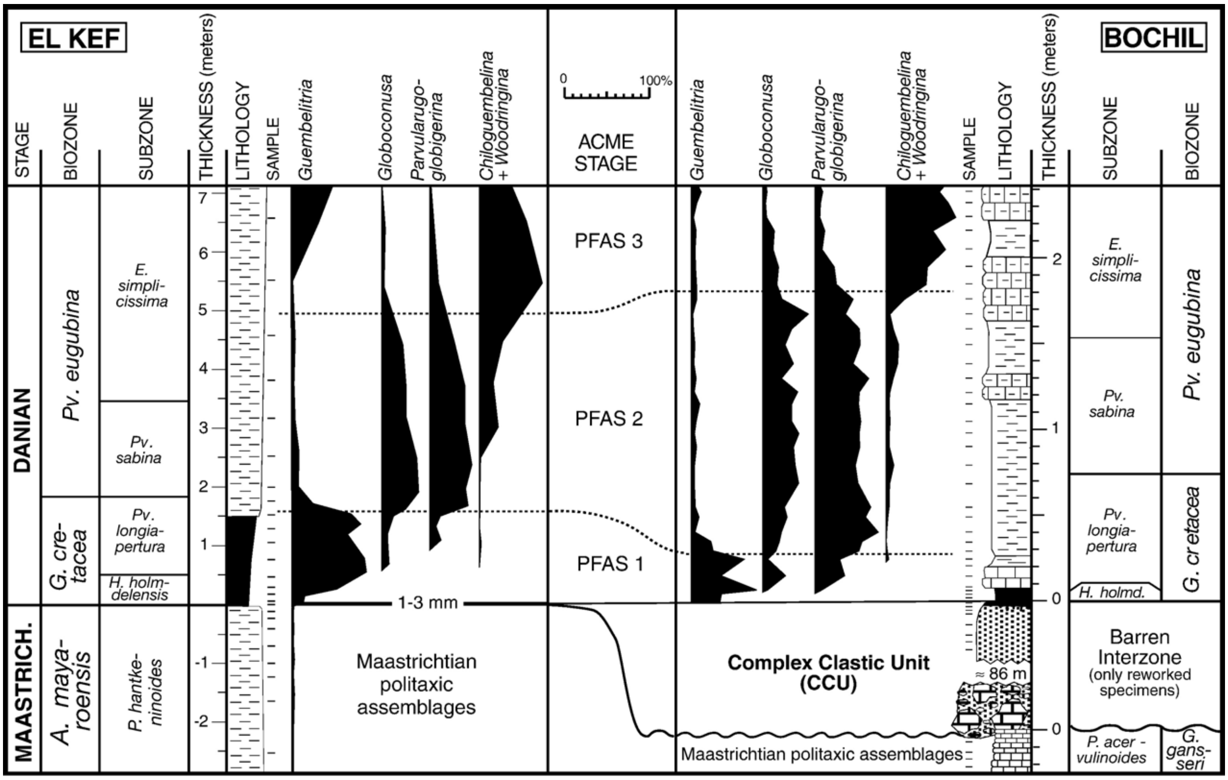

Fig. 5. Comparison of relative abundance of planktic foraminiferal groups and acme stages (PFAS) in the lowermost part of the Danian at Bochil and El Kef. The planktic foraminiferal assemblage turnovers are similar at both sections, although the sedimentation rates are different. The thick line at El Kef corresponds to the 1–3 mm-thick airfall layer, which is chronostratigraphically equivalent to the Bochil CCU. The lithological patterns are similar to what are indicated in the legend of Fig. 4.

section as an example that supports their interpretation [20,58,59]. Nevertheless, the age estimated by them for the Bochil CCU as well as their lithostratigraphic descriptions and sedimentological interpretations have changed over time. Firstly, they suggested that the breccia deposits equivalent to the CCU at Bochil are pre-K/Pg in age by considering that the uppermost meter of the CCU contains *P. hantkeninoides* and consists of "normal" Maastrichtian hemipelagic sand and shales deposited below the Ir-anomalous horizon [58]. Later, they proposed that this stratigraphical interval consists of brown shales and shaly marls containing planktic foraminiferal assemblages of the early Danian Subzone P1c [59]. Consequently, the Danian Biozones P0, P1a and P1b would be missing at Bochil, and the Ir-anomalous horizon would be the record of an early Danian impact event (Fig. 3 shows the correlation of their Danian biozonation [43] with the one used in the present paper). Finally, they suggested that the Ir anomaly, and consequently the early Danian impact event, is not in the Subbiozone P1c but in the Subbiozone P1a(1) [20]. This last suggestion was based on earliest Danian planktic foraminiferal species found in a "marly" level within the uppermost meter of the CCU. This interval was then re-described as a microconglomerate with altered spherules, bioturbated at the top, and placed below the Ir anomaly. Others also studied the Bochil and Guayal sections, concluding on the contrary that the Chicxulub-linked CCU is K/Pg in age [36–38]. Which is therefore the correct interpretation? Is it possible to utilize planktic foraminiferal data (high-resolution and quantitative biostratigraphy) to establish precisely the emplacement age of the CCU at Bochil and Guayal, and consequently the age of the Chicxulub impact event?

The erosional hiatus, linked to the CCU deposition, makes impossible to use the mass extinction biohorizon as the K/Pg key chronostratigraphic marker in the Gulf of Mexico and Caribbean sections [12,26,29,30]. Nevertheless, there are two ways to unravel this chronological problem at Bochil and Guayal using planktic foraminiferal data. The first one is to analyze the reworked planktic foraminiferal specimens in the CCUs, because it allows us to find out the latest age of the materials eroded and accumulated in these units. The second one is to analyze the micropaleontological record of the materials directly overlying CCUs, because the identification of the K/Pg boundary clay overlying the Chicxulub-related CCUs would provide solid proof of the age of the Chicxulub impact.

4.1. The Clastic Complex Unit

The CCU is also-called “K/Pg boundary cocktail” because it includes a distinctive mixture of reworked microfossils from different ages, impact-derived materials, and heterogeneous lithic fragments [35]. Although the reworked specimens cannot be used in biostratigraphic studies nor in the extinction pattern analysis, they can be utilized for the biochronological interpretations of the age of the CCU emplacement. In the CCU of the Bochil and Guayal sections (Tables 1 and 3), planktic foraminiferal specimens such as *Racemiguembelina powelli*, *Contusotruncana contusa*, *Pseudotextularia intermedia*, *Globotruncana linneiana*, *Contusotruncana fornicata* and *Pseudoguembelina hariaensis* were identified. These last three species have biochronological ranges that do not overlap in time (Fig. 3), indicating that the planktic foraminiferal assemblages identified in the CCUs are in fact reworked and mixed. The presence of *P. hariaensis* suggests that part of the eroded carbonate rock is late Maastrichtian in age, since the first appearance of *P. hariaensis* was approximately 1.8 Ma before the K/Pg boundary [44,60]. Furthermore, reworked specimens of *P. hantkeninoides* have also been identified in the Subunit 3 at Bochil [58]. The total range of this species spans approximately the latest 300 ka of the Maastrichtian [60], supporting the hypothesis that uppermost Maastrichtian facies were eroded in this area and accumulated in the local CCU. Such interpretation is compatible with the one that suggests a K/Pg age for the Chicxulub event.

Earliest Danian planktic foraminiferal species, including *P. eugubina* and *P. longiapertura*, have also been reported from the CCU at Bochil in a “marly” level placed 5–8 cm below the Ir-anomalous horizon, suggesting an early Danian age for this Ir anomaly [20]. Nevertheless, despite an exhaustive search, Danian species were not found in this level nor in any CCU sample at Bochil and Guayal. Those earliest Danian planktic foraminifera in Subunit 3 at Bochil could be infiltrated specimens by the bioturbation (*Chondrites*) on the top of the CCU.

4.2. The lowermost Danian

The most useful way to recognize the K/Pg boundary around the Gulf of Mexico is to identify the K/Pg boundary clay and the deposits equivalent to the airfall layer of El Kef, Caravaca and other continuous Tethyan sections. But, is the dark clay overlying the CCU at Bochil and Guayal equivalent to the K/Pg boundary clay? A positive answer to this question has been obtained by high-resolution planktic foraminiferal biostratigraphic studies like those used at the El Kef and Caravaca sections [12,22].

The lowermost centimeters of the dark clay bed at Bochil and Guayal, overlying the CCU at both sections, belong to the *H. holmdelensis* subzone (=Biozone P0) (Fig. 3). These biostratigraphic data were verified after identifying the typical oligotaxic planktic foraminiferal assemblages of that subzone, containing a few surviving Cretaceous species such as *G. cretacea* and *H. holmdelensis* (Tables 2 and 3). The top of the *H. holmdelensis* subzone is marked by the lowest stratigraphic records of the first Danian species to appear (*Globoconusa alticonusa* and *Parvularugoglobigerina longiapertura*), and is placed in the dark clay several centimeters above the CCU top (5 cm at Bochil, and 3 cm at Guayal).

The planktic foraminiferal acme stages shown in Fig. 5, especially the PFAS 1, can be used to further identify the K/Pg boundary clay and the continuity of deep environment sections in the Danian basal part since they do not involve problematic taxonomic assignments. The K/Pg boundary clay at El Kef and Caravaca contains a sudden bloom of opportunistic *Guembelitria* species, which helped to describe the PFAS 1 that spans a little more (the first 12–13 ka) than the K/Pg boundary clay (Figs. 4 and 5). The assemblages identified in the dark clay overlying the CCU at Bochil are also dominated by guembelitrids (*G. cretacea* and *G. trifolia*). This clay clearly belongs to the *H. holmdelensis* subzone (=Biozone P0) and PFAS 1, and is equivalent to the K/Pg boundary clay described at the El Kef stratotype.

Consequently, the thick Bochil and Guayal CCUs are chronostratigraphically equivalent to the El Kef and Caravaca millimeter airfall layers (Fig. 5), proving that they were deposited in one instantaneous geological event. The identification of the K/Pg boundary clay overlying the Chicxulub-linked CCU at Bochil and Guayal implies that this unit and the Chicxulub impact event are indeed K/Pg in age. Such data contradict the hypothesis that the Chicxulub impact event predates the K/Pg boundary by about 300 ka, and provides strong support that the K/Pg impact event and the Chicxulub impact event are the same one. Furthermore, there is no evidence at Bochil and Guayal for other impact events across the K/Pg boundary.

5. Conclusions

New detailed micropaleontological data from the Bochil and Guayal sections (SE Mexico) prove that the Chicxulub crater is precisely K/Pg boundary in age. The first, lowermost Danian *H. holmdelensis* subzone was identified in both sections in a dark clay bed just above the Complex Clastic Units that are genetically related to the Chicxulub impact. In addition, the *Guembelitria* acme (PFAS 1) was identified at Bochil after analyzing quantitatively the lowermost Danian planktic foraminiferal assemblages.

As a result, the dark clay bed overlying the Ir-anomalous horizon at Bochil and Guayal is equivalent to the K/Pg boundary clay, and the thick Clastic Complex Unit is chronostratigraphically equivalent to the millimeter airfall layer from the El Kef and Caravaca sections, at the base of which the K/Pg boundary was formally defined. The procedure described in this paper can be used to prove the continuity of K/Pg sections and provide a very precise biochronostratigraphic marker of the K/Pg boundary across the Gulf of Mexico and Caribbean sections.

Acknowledgments

We thank Alan R. Hildebrand and two other anonymous referees for the review of the manuscript. This research was funded by the project CGL2004-00738 of the Spanish Ministerio de Ciencia y Tecnología, by the Grupo Consolidado EO5 of the Gobierno de Aragón (Spain), and by the research project D.01003(2002–2004) of the Instituto Mexicano del Petróleo.

References

[1] L.W. Alvarez, W. Alvarez, F. Asaro, H.V. Michel, Extraterrestrial cause for the Cretaceous–Tertiary extinction, Science 208 (1980) 1095–1108.

[2] J. Smit, J. Hertogen, An extraterrestrial event at the Cretaceous–Tertiary boundary, Nature 285 (1980) 198–200.

[3] J. Smit, Meteorite impact, extinctions and the Cretaceous–Tertiary boundary, Geol. Mijnb. 69 (1990) 187–204.

[4] A.R. Hildebrand, W.V. Boynton, Proximal Cretaceous–Tertiary boundary impact deposits in the Caribbean, Science 248 (1990) 843–847.

[5] J. Smit, Extinction and evolution of planktonic foraminifera after a major impact at the Cretaceous/Tertiary boundary, Geol. Soc. Am. Spec. Pap. 190 (1982) 329–352.

[6] E. Robin, D. Boclet, P. Bonté, L. Froguet, C. Jéhanno, R. Rocchia, The stratigraphic distribution of Ni-rich spinels in Cretaceous–Tertiary boundary rocks at El Kef (Tunisia), Caravaca (Spain) and Hole 761C (Leg 122), Earth Planet. Sci. Lett. 107 (1991) 715–721.

[7] D.B. Carlisle, D.R. Braman, Nanometre-size diamonds in the Cretaceous/Tertiary boundary clay of Alberta, Nature 352 (1991) 708–709.

[8] A. Shukolyukov, G.W. Lugmair, Isotopic evidence for the Cretaceous/Tertiary impactor and its type, Science 282 (1998) 927–929.

[9] K.J. Hsü, J.A. McKenzie, 'Strangelove' ocean in the earliest Tertiary, Am. Geophys. Union–Geophys. Monograph 32 (1985) 487–892.

[10] J.W. Cowie, W. Zieger, J. Remane, Stratigraphic Commission accelerates progress, 1984–1989, Episodes 112 (1989) 79–83.

[11] J. Smit, T.B. Roep, W. Alvarez, A. Montanari, P. Claeys, J.M. Grajales-Nishimura, J. Bermudez, Coarse-grained, clastic sandstone complex at the K/T boundary around the Gulf of Mexico: deposition by tsunami waves induced by the Chicxulub impact? Geol. Soc. Am. Spec. Pap. 307 (1996) 151–182.

[12] I. Arenillas, J.A. Arz, E. Molina, C. Dupuis, An independent test of planktic foraminiferal turnover across the Cretaceous/Paleogene (K/P) boundary at El Kef, Tunisia: catastrophic mass extinction and possible survivorship, Micropaleontology 46 (2000) 31–49.

[13] G.T. Penfield, A. Camargo, Definition of a major igneous zone in the central Yucatan platform with aeromagnetics and gravity, Proc. 51th Annual Inter. Meeting, Soc. Exploration Geophys, 1981, p. 37.

[14] A.R. Hildebrand, G.T. Penfield, D.A Kring, M. Pilkington, A. Camargo, S.B. Jacobsen, W.V. Boynton, Chicxulub crater: a possible Cretaceous/Tertiary boundary impact crater on the Yucatan peninsula, Mexico, Geology 19 (1991) 867–871.

[15] V.L. Sharpton, G.B. Dalrymple, L.E. Marín, G. Ryder, B.C. Schuraytz, J. Urrutia-Fucugauchi, New links between the Chicxulub impact structure and the Cretaceous/Tertiary boundary, Nature 359 (1992) 819–821.

[16] C.C. Swisher III, J.M. Grajales-Nishimura, A. Montanari, P. Renne, E. Cedillo-Pardo, F.J.M.R. Maurrasse, G.H. Curtis, J. Smit, M.O. McWilliams, Chicxulub crater melt-rock and K–T boundary tektites from Mexico and Haiti yield coeval $^{40}Ar/^{39}Ar$ ages of 65 Ma, Science 257 (1992) 954–958.

[17] J.D. Blum, C.P. Chamberlain, M.P. Hingston, C. Koeberl, L.E. Marin, B.C. Schuraytz, V.L. Sharpton, Isotopic comparison of K/T boundary impact glass with melt rock from the Chicxulub and Manson impact structures, Nature 364 (1993) 325–327.

[18] T.E. Krogh, S.L. Kamo, V.L. Sharpton, L.E. Marin, A.R. Hildebrand, U–Pb ages of single shocked zircons linking distal K/T ejecta to the Chicxulub crater, Nature 366 (1993) 731–733.

[19] D.A. Kring, W.V. Boynton, Petrogenesis of an augite-bearing melt rock in the Chicxulub structure and its relationship to K/T impact spherules in Haiti, Nature 358 (1992) 141–144.

[20] G. Keller, W. Stinnesbeck, T. Adatte, D. Stüben, Multiple impacts across the Cretaceous–Tertiary boundary, Earth Sci. Rev. 1283 (2003) 1–37.

[21] W. Alvarez, F. Asaro, A. Montanari, Iridium profile for 10 million years across the Cretaceous–Tertiary boundary at Gubbio (Italy), Science 250 (1990) 1700–1702.

[22] I. Arenillas, J.A. Arz, E. Molina, A new high-resolution planktic foraminiferal zonation and subzonation for the lower Danian, Lethaia 37 (2004) 79–95.

[23] F.J.M.R. Maurrase, G. Sen, Impacts, tsunamis, and the Haitian Cretaceous–Tertiary boundary layer, Science 252 (1991) 1690–1693.

[24] J. Smit, A. Montanari, N.H.M. Swiburne, W. Alvarez, A.R. Hildebrand, S.V. Margolis, P. Claeys, W. Lowrie, F. Asaro, Tektite-bearing, deep-water clastic unit at the Cretaceous–Tertiary boundary in northeastern Mexico, Geology 20 (1992) 99–103.

[25] W. Alvarez, J. Smit, W. Lowrie, F. Asaro, S.V. Margolis, P. Claeys, M. Kastner, A.R. Hildebrand, Proximal impact deposits at the Cretaceous–Tertiary boundary in the Gulf of Mexico: a restudy of DSDP Leg 77 sites 536 and 540, Geology 20 (1992) 697–700.

[26] J.M. Grajales-Nishimura, E. Cedillo-Pardo, C. Rosales-Domínguez, D.J. Morán-Zenteno, W. Alvarez, P. Claeys, J. Ruíz-Morales, J. García-Henández, P. Padilla-Avila, A. Sánchez-Ríos, Chicxulub impact: the origin of reservoir and seal facies in the southeastern Mexico oil fields, Geology 28 (2000) 307–310.
[27] R. Tada, M.A. Iturralde-Vinent, T. Matsui, E. Tajika, T. Oji, K. Goto, Y. Nakano, H. Takayama, S. Yamamoto, S. Kiyokawa, K. Toyoda, D. García-Delgado, C. Díaz-Otero, R. Rojas-Consuegra, K/T boundary deposits in the paleo-western Caribbean basin, Am. Assoc. Pet. Geol. Mem. 79 (2003) 582–604.
[28] J.G. López-Oliva, G. Keller, Age and stratigraphy of near-K/T boundary siliciclastic deposits in northeastern Mexico, Geol. Soc. Am. Spec. Pap. 307 (1996) 227–242.
[29] J.A. Arz, I. Arenillas, A.R. Soria, L. Alegret, J.M. Grajales-Nishimura, C. Liesa, A. Mélendez, E. Molina, M.C. Rosales, Micropaleontology and sedimentology of the Cretaceous/Paleogene boundary at La Ceiba (Mexico): impact-generated sediment gravity flows, J. South Am. Earth Sci. 14 (2001) 505–519.
[30] L. Alegret, I. Arenillas, J.A. Arz, C. Díaz, J.M. Grajales-Nishimura, A. Meléndez, E. Molina, R. Rojas, A.R. Soria, Cretaceous/Paleogene (K/Pg) boundary clastic complex at Loma Capiro, Central Cuba: evidence for a K/Pg impact origin, Geology 33 (2005) 721–724.
[31] G. Keller, T. Adatte, W. Stinnesbeck, M. Rebolledo-Vieira, J. Urrutia-Fucugauchi, U. Kramar, D. Stüben, More evidence that the Chicxulub impact predates the K/T mass extinction, Meteorit. Planet. Sci. 39 (2004) 1127–1144.
[32] J.A. Arz, L. Alegret, I. Arenillas, Foraminiferal biostratigraphy and paleoenvironmental reconstruction at Yaxcopoil-1 drill hole (Chicxulub crater, Yucatan Peninsula), Meteorit. Planet. Sci. 39 (2004) 1099–1111.
[33] J. Smit, S. van der Gaast, W. Lustenhouwer, Is the transition impact to post-impact rock complete? Some remarks based on XRF scanning, electron microprobe, and thin section analyses of the Yaxcopoil-1 core in the Chicxulub crater, Meteorit. Planet. Sci. 39 (2004) 1113–1126.
[34] J. Bourgeois, T.A. Hansen, P.L. Wiberg, E.G. Kauffman, A tsunami deposit at the Cretaceous–Tertiary boundary in Texas, Science 241 (1988) 567–570.
[35] T.J. Bralower, C.K. Paull, R.M. Leckie, The Cretaceous–Tertiary boundary cocktail: Chicxulub impact triggers margin collapse and extensive sediment gravity flows, Geology 26 (1998) 331–334.
[36] S. Montanari, P. Claeys, F. Asaro, J. Bermudez, J. Smit, Preliminary stratigraphy and iridium and other geochemical anomalies across the KT boundary in the Bochil section (Chiapas, southeastern Mexico), Lunar Planet. Inst. Contr. Houston, vol. 825, 1994, pp. 84–85.
[37] J.M. Grajales-Nishimura, G. Murillo-Muñetón, C. Rosales-Domínguez, E. Cedillo-Pardo, J. García-Hernández, Heterogeneity of lithoclast composition in the deep-water carbonate breccias of the K/T boundary sedimentary succession, southeastern Mexico and offshore Campeche, Am. Assoc. Pet. Geol. Mem. 79 (2003) 312–329.
[38] R. Tagle, P. Claeys, Platinum group element (PGE) distribution in ejecta and impactites from Chicxulub, Abstract Book, 6th ESF-IMPACT Workshop "Impact Marker in the Stratigraphic Record", Granada, Spain, 2001, p. 129.
[39] J. Smit, The global stratigraphy of the Cretaceous–Tertiary boundary impact ejecta, Annu. Rev. Earth Planet. Sci. 27 (1999) 75–113.
[40] F. Lirer, A new technique for retrieving calcareous microfossils from lithified lime deposits, Micropaleontology 46 (2000) 365–369.
[41] W.A. Berggren, D.V. Kent, C.C. Swisher III, M.P. Aubry, A revised Cenozoic geochronology and chronostratigraphy, Soc. Econ. Paleontol. Miner. Spec. Pap. 54 (1995) 129–131.
[42] W.A. Werggren, P.N. Pearson, A revised tropical to subtropical Paleogene planktonic foraminiferal zonation, J. Foraminiferal Res. 35 (2005) 279–298.
[43] G. Keller, L. Li, N. MacLeod, The Cretaceous/Tertiary boundary stratotype section at El Kef, Tunisia: how catastrophic was the mass extinction? Palaeogeogr. Palaeoclimatol. Palaeoecol. 119 (1995) 221–254.
[44] J.A. Arz, E. Molina, Bioestratigrafía y cronoestratigrafía con foraminíferos planctónicos del Campaniense superior y Maastrichtiense de latitudes subtropicales y templadas (España, Francia y Tunicia), N. Jb. Geol. Paläont. Abh. 224 (2002) 161–195.
[45] M. Caron, Cretaceous planktic foraminifera, in: H.M. Bolli, J.B. Saunders, K. Perch-Nielsen (Eds.), Plankton Stratigraphy, Cambridge Univ. Press, 1985, pp. 17–86.
[46] M. Toumarkine, H.P. Luterbacher, Paleocene and Eocene planktic foraminifera, in: H.M. Bolli, J.B. Saunders, K. Perch-Nielsen (Eds.), Plankton Stratigraphy, Cambridge Univ. Press, 1985, pp. 88–153.
[47] S. Mukhopadhyay, K.A. Farley, A. Montanari, A short duration of the Cretaceous–Tertiary boundary event: evidence from extraterrestrial helium-3, Science 291 (2001) 1952–1955.
[48] I. Arenillas, J.A. Arz, E. Molina, C. Dupuis, The Cretaceous/Paleogene (K/P) boundary at Aïn Settara, Tunisia: sudden catastrophic mass extinction in planktic foraminifera, J. Foram. Res. 30 (2000) 202–218.
[49] J.A. Arz, I. Arenillas, E. Molina, R. Sepúlveda, La estabilidad faunística de los foraminíferos planctónicos en el Maastrichtiense superior y su extinción en masa catastrófica en el límite K/T de Caravaca, España, Rev. Geol. Chile 27 (2000) 27–47.
[50] L. Alegret, I. Arenillas, J.A. Arz, E. Molina, Foraminiferal event-stratigraphy across the Cretaceous/Tertiary boundary, N. Jb. Geol. Paläont. Abh. 234 (2004) 25–50.
[51] H. Leroux, R. Rocchia, L. Froget, X. Orue-Etxebarria, J-C. Doukhan, E. Robin, The K/T boundary at Beloc (Haiti): compared stratigraphic distributions of the boundary markers, Earth Planet. Sci. Lett. 131 (1995) 255–268.
[52] K.O. Pope, A.C. Ocampo, A.G. Fischer, W. Alvarez, B.W. Fouke, C.L. Webster, F.J. Vega, J. Smit, A.E. Fritsche, P. Claeys, Chicxulub impact ejecta from Albion Island, Belize, Earth Planet. Sci. Lett. 170 (1999) 351–364.
[53] P. Debrabant, E. Fourcade, H. Chamley, R. Rocchia, E. Robin, J-P. Bellier, S. Gardin, F. Thiébault, Les argiles de la transition Crétacé–Tertiaire au Guatemala, témoins d'un impact d'astéroïde, Bull. Soc. Geol. Fr. 170 (1999) 643–660.
[54] J.A. Arz, L. Alegret, I. Arenillas, C.L. Liesa, E. Molina, A.R. Soria, Extinción de foraminíferos del límite Cretácico/Terciario en Coxquihui (México) y su relación con las evidencias de impacto, Rev. Esp. Micropalaentol. 33 (2001) 221–236.
[55] A.R. Soria, C. Liesa, P. Mata, J.A. Arz, L. Alegret, I. Arenillas, A. Meléndez, Slumping and a sandbar deposit at the K/T boundary in the El Tecolote sector (northeastern Mexico): an impact-induced sediment gravity flow, Geology 29 (2001) 231–234.
[56] T.F. Lawton, K.W. Shipley, J.L. Aschoff, K.A. Giles, F.J. Vega, Basinward transport of Chicxulub ejecta by tsunami-induced backflow, La Popa basin, northeastern Mexico, and its implications for distribution of impact-related deposits flanking the Gulf of Mexico, Geology 33 (2005) 81–84.
[57] P. Schulte, R. Speijer, H. Mai, A. Kontny, The Cretaceous–Paleogene (K/P) boundary at Brazos, Texas: sequence stratigraphy, depositional events and the Chicxulub impact, Sediment. Geol. 184 (2006) 77–109.

[58] G. Keller, W. Stinnesbeck, Near-K/T age of clastic deposits from Texas to Brazil: impact, volcanism and/or sea-level lowstand? Terra Nova 8 (1996) 277–285.

[59] W. Stinnesbeck, G. Keller, T. Adatte, Chicxulub impact: the origin of reservoir and seal facies in the southeastern Mexico oil fields: comment, Geology 29 (2001) 94–95.

[60] L. Li, G. Keller, Diversification and extinction in Campanian–Maastrichtian planktic foraminifera of northwestern Tunisia, Eclogae Geol. Helv. 91 (1998) 75–102.

Table 1
Relative abundance (in %) of the uppermost Maastrichtian planktic foraminiferal species at Bochil (BK samples), and species identified in the Bochil CCU (BBr samples)

Species	Samples (cm)															
	BK −15 −20	BK −8 −10	BK −5 −7	BK −0 −3	BBr −8595 −8600	BBr −7960 −7965	BBr −6145 −6150	BBr −5815 −5820	BBr −4931 −4932	BBr −3540 −3541	BBr −2881 −2882	BBr −1765 −1760	BBr −1235 −1240	BBr −80 −85	BBr −5 −8	BBr −0 −3
Guembelitria cretacea		x	0.3	1.6								x			x	
Gb. trifolia	x		x	0.3												
Heterohelix planata	0.9	2.6	2.5	3.8												x
H. globulosa	39.7	40.6	41.6	38.9	x	x	x				x	x		x		
H. pulchra	0.6	1.3	1.6	1.9			x						x			x
H. punctulata	x	0.3	0.9	0.6												
H. navarroensis	8.5	9.4	7.3	6.3		x				x						
H. labellosa	9.1	5.2	8.5	8.9					x		x				x	
Pseudotextularia nuttalli	1.3	1.0	0.9	0.3	x			x								
P. elegans	x	x	x	x										x		
P. intermedia	x	x						x					x		x	
Racemiguembelina powelli						x									x	
Gublerina acuta	x	x	x													
G. cuvillieri		x														
Pseudoguembelina kempensis	0.3	x	x													
P. palpebra	x	0.3	x	x												x
P. costulata	5.4	7.1	5.7	6.3									x		x	
P. costellifera	x		x											x		
P. excolata	x	x	x	x												
P. hariaensis								x							x	
Planoglobulina acervulinoides	x	x	x													
P. carseyae	x	x	0.3	x				x								
P. riograndensis	x	x														
P. multicamerata	x	x		x												
Globigerinelloides yaucoensis	3.2	3.5	2.8	2.5		x			x							
G. rosebudensis	0.3	0.3	0.9	0.3												
G. prairiehillensis	7.6	8.1	4.7	3.8				x		x					x	
G. volutus	5.4	2.6	3.8	3.2												
G. subcarinatus	x	0.3	0.9	0.6			x									x
Hedbergella monmouthensis	3.2	2.9	5.4	4.1	x			x		x						
H. holmdelensis	6.3	7.4	5.0	7.0		x	x									x
Globotruncanella havanensis	x	0.3	0.3	x												
G. petaloidea	x	x	0.6	0.3		x					x					
G. pschadae	x	x		x												
Archaeoglobigerina cretacea	0.3	0.6	x	0.6												
A. blowi		x	x	0.3												
Rugoglobigerina rugosa	1.9	1.3	1.6	2.8	x										x	

Table 1 (*continued*)

Species	Samples (cm)															
	BK	BK	BK	BK	BBr	BBr	BBr	BBr	BBr	BBr	BBr	BBr	BBr	BBr	BBr	BBr
	−15	−8	−5	−0	−8595	−7960	−6145	−5815	−4931	−3540	−2881	−1765	−1235	−80	−5	−0
	−20	−10	−7	−3	−8600	−7965	−6150	−5820	−4932	−3541	−2882	−1760	−1240	−85	−8	−3
R. hexacamerata	0.6	x	x	0.3		x										
R. scotti	x	x	x	x		x										
R. pennyi	x	x	x	x							x					
R. macrocephala	x		x	x					x						x	
Globotruncana arca	1.6	1.6	1.6	1.9		x										
G. aegyptiaca	0.3	0.6	0.3	0.6				x								
G. linneiana	x	x		x												
G. orientalis	x	x	x	x												
G. mariei	2.2	1.3	1.9	1.3	x											x
G. falsostuarti		x	x	x												
G. bulloides	x	0.3	x	x												
Globotruncanita stuarti	x	x	x					x								x
G. stuartiformis	x	0.3	x	x										x		
G. insignis	x	x	x	x												
G. fareedi	0.6	0.6	0.3	0.9		x										
G. dupeublei	x	x	x	x												
G. angulata		x	x													
Contusotruncana contusa			x					x						x		
C. walfischensis	x	x														
C. patelliformis	0.3	x		x												
C. fornicata	x	x	x	0.3										x		
C. plummerae	0.3	x	x	x												
Gansserina wiedenmayeri	x	x														
Abathomphalus intermedius	x	x		x												
Total picked specimens	317	310	317	316												

The BK samples are numbered in cm from the K/Pg boundary downward. The BBr samples are numbered in cm from the top of the CCU downwards ("x" indicates that the species was found in the sample after an intensive search). In addition to the 16 samples shown in the table, we analyzed another 11 samples, but none contained planktic foraminifera.

Table 2
Relative abundance (in %) of lowermost Danian planktic foraminiferal species at Bochil (BP samples)

Species	BP	BP	BP	BP	BP	BP	BP	BP	BP	BP	BP	BP	BP	BP	BP
	+0	+2	+4	+14	+24	+30	+33	+38	+45	+50	+65	+77	+85	+95	+100
	+2	+4	+6	+16	+26	+32	+35	+40	+50	+55	+70	+82	+90	+100	+105
Parvularugoglobigerina longiapertura			2.7	15.0	2.5	9.0	15.6	16.2	19.3	20.7	6.5	12.0	18.8	17.8	14.8
P. perexigua			2.7	5.8	2.5	3.7	3.9	3.2	5.6	3.6	35.0	24.7	11.1	18.4	12.9
P. umbrica			1.0	2.4	x	4.0	1.3	1.4	0.7	x	x	1.5	0.3	x	0.3
P. eugubina													2.6	3.6	4.5
P. cf. hemisphaerica															
P. sabina					0.9	0.7	x	1.7	3.3	2.4	0.7	0.6	4.1	2.4	2.3
Globoconusa alticonusa			3.7	17.9	10.5	28.0	42.7	34.4	5.6	8.4	1.6	2.7	7.6	3.6	5.5
G. fodina			1.7	6.8	8.3	11.7	7.5	25.7	24.8	22.5	18.6	16.3	7.6	10.9	11.9
G. minutula			2.3	2.9	4.9	4.0	4.6	3.8	12.7	16.5	22.9	16.0	7.0	3.9	9.0
G. extensa						1.3	x	0.3	0.3	0.9	x	0.6	0.6	1.8	1.3
G. cf. fringa				4.3	6.2	6.3	1.6	9.8	16.3	18.0	8.5	12.7	30.2	31.7	26.7
Eoglobigerina simplicissima															
E. eobulloides															
E. fringa															
E. microcellulosa															
E. praeedita															
E. trivialis															
Parasubbotina moskvini															
P. pseudobulloides															
Praemurica taurica															
P. pseudoinconstans															
Globanomalina archeocompressa															
G. imitata															
G. planocompressa															
Chiloguembelina morsei									0.7	0.3	1.3	2.4	1.5	2.1	2.3
C. midwayensis									0.3	0.9	0.7	3.3	0.6	0.3	1.3
Woodringina claytonensis					0.3	0.3	x	x	0.3	0.6	x	0.6	x	x	x
W. hornerstownensis					1.8	0.7	x	0.3	0.3	1.2	1.3	3.3	1.2	0.6	1.0
Guembelitria danica	1.7	1.7	1.7	2.4	0.3	0.7	1.3	0.3	0.7	x	x	0.3	0.9	0.3	1.6
G. irregularis	x	1.3	1.7		1.8	1.0	1.3	x	0.7	0.9	0.3	0.6	0.6	0.3	0.6
G. cretacea	21.2	15.2	40.2	18.4	26.5	18.0	13.0	2.6	5.6	2.7	2.3	2.1	4.7	1.8	3.9
G. trifolia	11.0	22.4	34.2	20.3	32.9	8.3	7.2	0.3	2.3	0.6	0.3	0.3	0.6	0.3	0.3
Heterohelix planata	0.3	2.6	x		0.3										
H. globulosa	34.6	22.8	4.0	1.9	x	0.3	x	x	0.3	x					
H. navarroensis	4.7	1.3	0.3												
Pseudoguembelina costulata	x	3.0													
Globigerinelloides yaucoensis	1.2	5.0	0.7	0.5											
G. prairiehillensis	2.0	4.6	0.3												
G. volutus	2.6	5.3													
G. subcarinatus	0.9														
Hedbergella monmouthensis	6.7	4.0	2.0	0.5	x	1.0									
H. holmdelensis	12.5	6.9	1.0	1.0	0.3	1.0	x		0.3						
Other Cretaceous species	0.6	4.0													
Total picked specimens	344	303	301	207	325	300	307	346	306	334	306	332	341	331	311
Guembelitria	34.0	40.6	77.7	41.1	61.5	28.0	22.8	3.2	9.2	4.2	2.9	3.3	6.7	2.7	6.4
Parvularugoglobigerina			6.3	23.2	5.8	17.3	20.8	22.5	28.8	26.6	42.2	38.9	37.0	42.3	34.7
Globoconusa			7.6	31.9	29.8	51.3	56.4	74.0	59.8	66.2	52.6	48.2	53.1	52.0	54.3
Chilog.+Wood.					2.2	1.0	x	0.3	1.6	3.0	3.3	9.6	3.2	3.0	4.5
Other Paleocene genera															

The BP samples are numbered in cm from the top of the CCU upward ("x" indicates that the species was found in the sample after an exhaustive search). In addition to the 31 samples shown in the table, we analyzed another four samples, but none contained planktic foraminifera.

BP	BP	BP	BP	BP	BP	BP	BP	BP	BP	BP	BP	BP	BP	BP	BP
+111	+118	+128	+135	+145	+155	+163	+173	+183	+192	+202	+212	+218	+228	+235	+240
+116	+123	+133	+140	+150	+160	+168	+178	+188	+197	+207	+217	+223	+233	+240	+245
13.5	14.2	4.8	7.3	10.4	7.6	20.0	1.9	2.6	0.6						
14.1	16.0	9.7	19.7	7.4	8.2	11.5	0.9	0.7							
x	0.3	x	0.3												
5.0	6.6	5.1	4.8	7.0	12.0	17.0	13.4	10.5	16.1	9.0	10.0	2.5	1.9	2.6	1.6
								x	0.3	0.3	0.6	0.3	0.3	0.7	x
2.1	3.8	2.4	4.8	2.7	6.4	5.8	5.9	3.9	2.6	2.5	2.9	2.0	0.6	2.0	1.6
7.1	7.5	14.2	8.3	10.7	16.9	9.1	13.8	3.9	5.8	3.1	2.3	1.1	1.3	2.0	1.0
14.7	10.7	18.0	15.6	13.7	17.5	11.2	9.1	7.8	4.5	1.6	0.6	1.1	1.0	1.0	1.0
5.6	10.1	12.1	4.1	8.7	3.5	4.5	5.9	5.6	5.1	0.6	1.9	0.6	0.6	1.7	1.0
0.3	0.3	1.1	1.0	x	0.3	1.5	0.6	x	x	x	x	x	0.6	0.7	0.3
24.1	23.6	18.0	17.5	20.4	14.6	10.6	16.3	8.8	8.0	4.0	7.1	3.6	3.2	4.3	3.0
					0.3	0.3	0.9	1.0	0.6	0.6	1.3	1.4	2.2	1.7	1.6
					0.3	0.9	0.9	0.3	0.6	0.6	0.6	0.6	0.6	x	0.3
												0.3	x	1.0	0.7
											0.3	0.6	0.3	0.3	1.0
										x	1.3	0.3	0.6	1.3	1.3
														0.3	0.3
										0.6	3.2	0.6	3.2	3.0	2.0
															1.0
											2.6	x	1.3	1.0	1.6
															1.3
					1.2	1.5	0.9	0.7	1.0	0.6	2.9	x	0.6	1.3	0.3
						0.3	0.3	x	0.3	0.9	1.3	0.6	0.3	0.7	x
										0.3	x	x	1.0	0.3	x
1.5	1.3	3.0	1.9	3.0	3.2	1.2	1.3	6.5	2.3	1.6	2.9	15.4	2.5	3.0	2.6
1.8	1.3	2.2	3.5	3.3	2.0	0.6	x	1.3	x	0.3	0.3	2.8	1.3	1.7	0.7
x	0.3	0.3	0.6	0.7	0.3	0.3	0.6	1.6	2.6	4.7	3.2	3.9	6.7	5.9	5.9
0.3	0.9	3.2	7.3	7.7	3.5	2.1	20.3	37.9	44.4	63.9	48.7	60.6	63.2	52.1	63.3
2.1	0.3	0.3	0.6	x	x	x	x	x	0.3	0.9	x	0.3	x	0.7	0.3
x	0.3	x	0.3	0.3	0.3	0.3	0.6	3.3	1.6	1.6	0.3	x	0.6	1.7	0.3
6.8	2.2	3.5	2.2	3.3	0.6	0.9	5.3	2.6	1.6	1.9	4.5	1.7	5.1	6.6	4.6
1.2	0.3	2.2	0.3	0.7	1.5	0.3	0.9	1.0	1.6	0.3	1.0	x	1.0	2.6	1.3
340	318	372	315	299	343	330	320	306	311	321	310	358	315	303	305
10.0	3.1	5.9	3.5	4.3	2.3	1.5	6.9	6.9	5.1	4.7	5.8	2.0	6.7	11.6	6.6
34.7	40.9	22.0	36.8	27.4	34.1	54.2	22.2	17.6	19.6	11.8	13.5	4.7	2.9	5.3	3.3
51.8	52.2	63.4	46.3	53.5	52.8	37.0	45.6	26.1	23.5	9.3	11.9	6.4	6.7	9.6	6.2
3.5	3.8	8.6	13.3	14.7	9.0	4.2	22.2	47.4	49.2	70.4	55.2	82.7	73.7	62.7	72.5
					1.7	3.0	3.1	2.0	2.6	3.7	13.5	4.2	10.2	10.9	11.5

Table 3
Species identified in the uppermost Maastrichtian (GK samples), CCU (GBr samples) and lowermost Danian (GP samples) at Guayal ("x" indicates that the species was found in the sample after an intensive search)

Species	Samples (cm)																					
	GK	GK	GK	GBr	GBr	GBr	GBr	GBr	GBr	GP	GP	GP	GP	GP	GP	GP	GP	GP	GP	GP	GP	GP	GP
	−195	−45	−0	3655	−2592	−1295	−1195	−610	−0	+0	+1	+3	+5	+19	+24	+45	+62	+67	+70	+75	+85	+90	+100
	−200	−50	−3	−3660	−2600	−1300	−1200	−615	−3	+1	+3	+5	+7	+24	+32	+47	+67	+70	+75	+80	+90	+95	+105
Guembelitria cretacea										x	x	x		x	x		x		x	x	x		x
G. trifolia		x								x	x	x					x						
Heterohelix planata	x	x	x																				
H. globulosa	x	x	x	x	x		x	x		x	x	x											
H. pulchra	x		x																				
H. punctulata	x		x																				
H. navarroensis	x	x	x						x														
H. labellosa	x	x	x	x		x																	
H. postsemicostata		x	x																				
Pseudotextularia nuttalli	x	x	x		x																		
P. elegans		x																					
P. intermedia	x				x	x																	
Racemiguembelina powelli				x					x														
R. fructicosa			x																				
Pseudoguembelina kempensis	x	x	x																				
P. costulata	x	x	x				x			x													
P. excolata		x																					
P. hariaensis				x		x		x															
Planoglobulina acervulinoides	x		x																				
P. carseyae		x	x				x																
P. multicamerata	x		x	x																			
Globigerinelloides yaucoensis	x	x	x							x													
G. rosebudensis			x																				
G. prairiehillensis	x	x	x							x	x		x										
G. volutus	x	x	x		x					x													
Hedbergella monmouthensis	x	x	x	x						x	x	x											
H. holmdelensis	x	x	x			x			x	x	x												
Globotruncanella havanensis		x	x					x															
G. minuta	x	x	x																				
Archaeoglobigerina cretacea		x	x																				
A. blowi	x		x																				
Rugoglobigerina rugosa	x	x	x	x																			
R. hexacamerata	x	x	x				x																
R. scotti	x	x	x																				
R. reicheli	x		x																				
Globotruncana arca	x	x	x	x																			
G. aegyptiaca	x	x	x																				

G. linneiana	x	x	x		x													
G. mariei	x	x	x			x												
G. falsostuarti		x	x															
G. bulloides	x	x	x															
G. ventricosa	x		x															
G. stuartiformis		x	x	x														
G. fareedi	x																	
Contusotruncana contusa	x		x	x														
C. patelliformis			x															
C. fornicata	x	x	x															
C. plummerae		x																
Parvularugog. longiapertura							x	x	x	x	x	x		x				
P. perexigua							x		x	x	x	x		x				
P. umbrica							x			x		x						
P. eugubina									x		x	x		x	x	x	x	x
P. cf. *hemisphaerica*												x						x
P. sabina									x			x		x	x	x	x	x
Globoconusa alticonusa							x		x	x	x	x		x	x			x
G. fodina							x		x	x		x	x	x		x		
G. minutula							x			x		x		x				x
G. extensa									x			x						
G. cf. *fringa*							x		x			x		x	x	x	x	x
Eoglobigerina simplicissima												x		x				x
E. eobulloides														x				
E. microcellulosa																		x
E. praeedita																		x
Parasubbotina moskvini																		x
P. pseudobulloides																		x
Praemurica taurica																		x
P. pseudoinconstans																		x
Globanomalina archeocompressa														x		x		x
Chiloguembelina morsei												x		x	x	x		x
C. midwayensis												x			x	x		
Woodringina claytonensis													x	x	x			x
W. hornerstownensis							x		x		x	x		x	x	x		x
Guembelitria danica																		x
G. irregularis									x					x	x		x	x

The GK samples are numbered in cm from the K/Pg boundary downward. The GBr samples are numbered in cm from the top of the CCU downward. The GP samples are numbered in cm from the top of the CCU upward. In addition to the 23 samples shown in the table, we analyzed another 31 CCU samples and 6 lowermost Danian samples, but none contained planktic foraminifera.